

LD Benchmark

Report

- I - LD BENCHMARK: BACKGROUND AND GOALS.....	2
- II - INFORMATION ON RESULTS	3
- III - DETERMINISTIC OR CHAOTIC BEHAVIOR.....	4
- IV - TRACK FOUNDATION	5
- V - PARTICIPANTS	6
- VI - DATA VERIFICATION.....	7
- VII - RESULTS	8
- VII.1 CASE 1 - SIMPLIFIED “S” PROFILES	8
- VII.1.1 Exercise 3S: initial lateral velocity = 1m/s.....	8
Displacements	8
Normal forces.....	9
- VII.1.2 Exercise 4S: initial lateral velocity = 2m/s.....	13
Displacements	13
Normal forces.....	13
- VII.2 CASE 1 - ACTUAL “A” PROFILES	17
- VII.2.1 Exercise 3A: initial lateral velocity = 1m/s	17
Displacements	17
Normal forces.....	17
- VII.2.2 Exercise 4A: initial lateral velocity = 2m/s	22
Displacements	22
Normal forces.....	22
- VIII - First Impact Details.....	26
- IX - CONCLUSIONS	27
ANNEX 1 - BENCHMARK DATA -.....	28
ANNEX 2 - CODES STATUS -	33
ANNEX 3 - HERTZ FORMULA -	34
ANNEX 4 – ELLIPTIC INTEGRALS REFINED TABLES	36

These Benchmark exercises were at first presented at the Long Beach ASME Railway Symposium in September 2005 and were published on the VOLPE Web Site at the following address:

<http://www.volpe.dot.gov/sdd/ldbenchmark.html>

- I - LD BENCHMARK: BACKGROUND AND GOALS

The LD Benchmark relates to the broad field of dynamic simulation of railway vehicles and specifically to one fundamental feature, namely calculation of wheel/rail contact forces in the direction normal to contact patches. From its inception, the aim of this benchmark was to analyze normal contact force calculations and modeling of flanging with impacts. This benchmark problem involves computation of contact forces resulting from elastic impact of wheel flanges with stiff track. These conditions are typically associated with higher speed derailments.

There are a number of railway codes available to simulate vehicle behavior to assess derailment risks in critical higher speed situations. In comparing these codes, differences have been observed in the forces and displacements as well as in the likelihood of prediction of derailment. The intent of the LD Benchmark is to understand how different modeling assumptions influence the results, and to promote technology transfer in order to produce more consistent predictions using these codes.

Attempts have also been made to compare physical onboard train measurements to simulations to verify validity of codes. However, this approach did not explain the shortcomings of different modeling methodologies and did not always provide sufficient insight for their improvement.

Several previous railway benchmarks have already been conducted. Due to the complexity of the models used in these benchmarks and their numerous simplifying assumptions, it was difficult to understand the source of differences in their predicted results and the extent to which the simplifying assumptions have contributed to such differences. As a consequence, it was suggested that a new benchmark which utilizes a more fundamental model could be more useful, even if such a benchmark may not be fully reflective of a realistic condition.

The new suggested benchmark, which is the focus of this report, uses a single unsuspended wheelset loaded with a constant vertical force, running on an idealized frictionless and rigid perfect track (the call for simulations and full problem description announced at the Long Beach Railway Symposium in September 2005 is given in Annex 1). The elimination of wheelset suspension avoids the need for calculating sprung mass response and its compounding contribution to wheel rail contact. Similarly, the idealization of track as frictionless and rigid eliminates the compounding effects of factors such as tangential forces and track response on wheel rail contact.

While in principle it could have been possible to isolate treatment of wheel rail contact using quasi-static calculations (as in the case of the Herbertov-Pascal-Benchmark), the proposed benchmark was deemed more beneficial to allow for the inclusion of simulation codes that exclusively utilized rigid contact and to gage the influence of dynamic variations. It was expected to find different force results due to differences in coding assumptions. In addition, differences in wheel/rail impact forces that otherwise could seem negligible are expected to produce displacement bifurcations (see Chapter III).

- II - INFORMATION ON RESULTS

Results from seven participants (see Chapter V) had been received by the Benchmark deadline of June 16 2006. The Federal Railroad Administration/French Ministry of Transportation (FRA/DTT) Cooperation Team reviewed the submitted data and published the results of all participants for one exercise on the VOLPE Web Site.

Six of the seven simulations used elastic Hertzian contacts; the seventh, VAMPIRE, used a rigid algorithm together with linear elasticity between wheel and ground.

Although a rigid track was requested in the Benchmark specification, initially two participants, NUCARS and VAMPIRE, could not simulate a rigid track and were using some elasticity between wheelset and ground. Initially, results of these two codes were different from the other five which were using a rigid track together with elastic Hertzian wheel/rail contact methods.

In the meantime, the NUCARS team developed their code in order to be able to simulate wheelsets using an elastic Hertzian model on rigid tracks and proposed new results that match very well with the others.

Although VAMPIRE did not modify their code, they proposed new results with increased track lateral stiffness (from $3E9$ to $100E9$ N/m) and enlarged their contact data table using a wider lateral shift relative to the rails of ± 80 mm. To produce the new VAMPIRE results, they “further stiffened the track model in the VAMPIRE analysis to match the impulses from the elastic codes. The track flexibility in VAMPIRE was set to match the elastic contact between wheel and rail, but this can only be achieved for the first impact which is predictable.” As a result, “subsequent impact forces in VAMPIRE tended to be higher than those predicted by the elastic codes.”

In addition, in this Benchmark some small differences between Hertzian codes were analyzed and it appeared that the greatest part of it came from differences in either using various tables or direct integration (DYNARAIL) for calculating elliptic integrals that are necessary in Hertzian methods. Some tables (notably tables published by Hertz himself) did not have enough data to be properly interpolated. Thus, more refined tables were calculated during the summer and were used by SAMSRAIL and VOCODYM+ that also accordingly issued new results.

In addition, six out of seven results for one case with simplified profiles showed wheelset lateral displacement clearly tending toward derailment, which raised interest in increasing the simulation time to further investigate this derailment possibility. All participants agreed to verify this assumption by increasing this simulation time up to 200 ms and produced new results that show derailment conditions for this case.

Considering that the cooperative discussions initiated by this benchmark produced these new developments that were real improvements in the field of railway modeling, and additionally that participants agreed to publish the new results, the LD Benchmark team decided to issue this report taking into account the new results and comments, as received early in November 2006.

- III - DETERMINISTIC OR CHAOTIC BEHAVIOR

When severe impacts occur, wheel-rail dynamics can be difficult to predict mainly because of the high stiffness of steel on steel contact inducing non-smooth behavior. For this reason, chaotic behavior is expected, and deterministic displacements should not occur over a long range of time. The chaotic nature of the problem will appear when very small modifications, for instance smaller than measurement accuracy, dramatically change the results. Thus, when severe ride conditions occur, it is not expected to obtain the same displacements under conditions that appear to be nearly identical.

If using different codes to simulate the same case produces results that are different from the very beginning of the simulation, the problem is chaotic and/or the actual mechanism is so complicated that different simplifying hypotheses are used in each code. But there probably would remain doubts of unrealistic simulations. This did not happen for this benchmark.

If the results are only diverging slowly with time, which is the case here, it can be said that the simulations are accurate and deterministic up to a certain time and look less deterministic over longer times. However, for these simulations dealing with relatively simple mechanisms allowed participants to improve their modeling hypotheses in order to improve correlations between results and thus reach a consensus on the best possible model and best way of programming. This is one of the benefits of this benchmark.

Once a sound model is assessed in this manner, the nature of the problem is such that differences between results of different codes will nevertheless be observed after some time. Such long chaotic simulations are not meaningless but the results (derailment risks for instance) must be understood statistically.

Six of the seven results of case 3S (lateral initial velocity = 1m/s), all of them using elastic Hertzian contacts and rigid track without damping, have nearly identical results for the 100ms duration of the simulations which means very close modeling hypotheses and very robust numerical treatment in these codes.

These similarities in prediction of wheelset behavior, gained using codes being developed independently, tend to drive the conclusion that they all have implemented the theory correctly since they get nearly identical results. The question on whether Hertz theory is appropriate to solve these wheel/rail mechanisms remains open. In the meantime this theory can be said to be at least “deterministic” for this exercise during the initial 100ms.

As discussed in Chapter VII, the displacement differences in exercise 3S that appeared in the June results for two of the seven codes have now been eliminated. These differences were caused by elasticity in track models. NUCARS results using rigid track are now identical and VAMPIRE displacements, having adjusted lateral elasticity, are now similar although the contact forces remain different.

In exercise 3A using actual wheel and rail profiles, differences in the June results appeared more quickly for all codes. These differences were thought to be linked to the fact that in this case of actual profiles, curvatures and contact angles are varying along contact situations, which implies approximations when using Hertz formula. New results, using refined tables for elliptic integrals are now quite similar.

- IV - TRACK FOUNDATION

The modeling of wheel and rail interaction is a complex task involving many physical and analytical considerations. As stated in Chapter I, the aim of this benchmark was to analyze normal contact force calculations and modeling of flanging with impacts. This benchmark problem involves computation of contact forces resulting from elastic impact of wheel flanges with stiff track which implies models that account for the capture and release of a wheel, high energy transfer during impact, and response to stiff track. These forces between the wheel and rail result from elastic deformation at the contact patch.

The benchmark problem was designed to compare calculation of contact forces without the influence of any damping or additional elasticity other than that provided by wheel and rail contact. The elimination of damping and track foundation stiffness enables focusing on the influence of contact stiffness between the wheel and rail. This contact stiffness is nonlinear and characterized by the shape of the contact patch and curvature at the point of contact, which vary as the wheelset is displaced across the track. In six of the seven codes, the interaction of the wheel and rail is represented as a Hertzian contact spring which allows loss of contact between the wheel and rail and gives a nonlinear contact stiffness that is a function of the curvature of the wheel and rail at the contact point. The remaining code, VAMPIRE, uses a track foundation model to represent the combined effects of contact stiffness and track foundation stiffness. This track foundation model, which is linear and independent of variations in wheel and rail contact geometry, is used to compute the normal contact force between the wheel and rail.

In two of the codes, a track foundation model was an integrated component of the model between wheel and ground. It was proposed to include a track foundation model in this benchmark problem. In the first code, NUCARS, a method had to be developed for simulating rigid (infinite stiffness and no damping) rails when using a Hertzian contact spring model. In the second code, VAMPIRE, it was necessary to keep the track foundation model in order to compute the contact forces as described above. While modeling the effects of track foundation is useful and important, the current Benchmark was intended to focus on the challenges associated with modeling the nonlinear contact spring and the forces developed during flange impact. A model which includes the mass and stiffness associated with the track foundation is needed in order to study the influence of track properties on wheel rail contact forces. However, this exercise is proposed to be the subject of a future benchmark.

- V - PARTICIPANTS

New results of seven participants have now been received in early November 2006 and have been reviewed by the FRA/DTT Cooperation Team.

Annex 2 is a listing of the seven codes status. Detailed information about the codes is provided in attached files. The main characteristics of the codes are as follows:

DYNARAIL –

Contact: Dr. Jalil Sany <jrsany@ameritech.net>

Contact method: Hertzian (Kalker's formula & refined elliptic tables) – friction=0

Track suspension: rigid and un-damped

LDYN –

Contact: Prof. Claude Bohatier <bohatier@lmgc.univ-montp2.fr>

Contact method: Hertzian (Hertz's formula & Courbon tables) – friction=0

Track suspension: rigid and un-damped

NUCARS –

Contact: Nicholas Wilson <nicholas_wilson@aar.com>

Contact method: Multi-Hertzian philosophy – friction = very small

Track suspension: rigid and un-damped:

SAMSRAIL –

Contact: Dr. Khaled Zaazaa <zaazaa.khaled@ensco.com>

Contact method: Hertzian (Hertz's formula and refined tables) – friction=0

Track suspension: rigid and un-damped

SIMPACK –

Contact: Dr. Christoph Weidemann <Christoph.Weidemann@simpack.de>

Contact method: Hertzian – friction=0

Track suspension: rigid and un-damped

VAMPIRE –

Contact: Alan Minnis <Alan.Minnis@deltarail.com>

Contact method: Rigid, low friction (0.0001)

Track suspension: semi-rigid and un-damped:

100000 kN/mm - Vertical rail to ground

3000 kN/mm - Lateral rail to sleeper

100000 kN/mm - Lateral sleeper to ground

No Track Damping

VOCODYMPLUS –

Contact: Dr. Jean-Pierre Pascal <pascal.voc@wanadoo.fr>

Contact method: Hertzian (Hertz's formulae and refined tables) – friction=1E-15

Track suspension: rigid and un-damped

Track mass = 1E+15 kg All stiffnesses > 1E+15 N/m Track damping = 0

This short list above allows classifying the codes into 2 types:

A - ELASTIC HERTZIAN CONTACT + RIGID UN-DAMPED TRACK:

- DYNARAIL
- LDYN
- SAMSRAIL
- SIMPACK
- VOCODYMPLUS
- NUCARS

B – RIGID CONTACT LINEAR ELASTICITY PROVIDED BETWEEN WHEEL AND GROUND:

- VAMPIRE

- VI - DATA VERIFICATION

Before publishing the report on the web site, it was verified that the results were correctly understood and that the Benchmark data were the same for all simulations.

Due to the chaotic nature of the problem very small modifications in the data, such as adding a few micrometers in the track gage or slightly smoothing the profiles, could change the results significantly after some time. Thus several items were to be reviewed in order to minimize potential causes of differences between simulations:

Gage Point Height

It was necessary for all participants to verify that they have set the track gage at the same imposed height of 14mm below the top of rail.

Smoothing Procedures

Participants were asked to describe any specific procedures that were used for smoothing the profiles.

Material Properties

Participants were asked to provide the values used for the steel elastic properties. All participants did not use the same steel elastic properties. It was not specified in the benchmark data assuming that most of the codes used $E=210000\text{N/mm}^2$, $\nu=0.28$.

VAMPIRE noted using $E=200000\text{N/mm}^2$, $\nu=0.30$, but not for calculating normal forces.

Initial System Energy

Not all results calculated the same initial system energy (initial potential energy is arbitrary). For further reports we decided to interpret all results in order to have the same initial energy (zero) and to plot only the variations of the sum.

Contact Positions & Angles

Contact positions and contact angles references are not the same in all codes. Some are with respect to wheelset and others to track. To present comparable results (track frame), it was necessary to make modifications.

- VII - RESULTS

The four exercises of case 1 entailed simulating wheelset behavior from an initial centered vertical equilibrium with various initial lateral velocities to force the wheelset towards an impact against left rail.

These initial velocities were:

Exercise	1	2	3	4
Initial Velocity	0.1 m/s	0.5 m/s	1 m/s	2 m/s

After reviewing the large number of results submitted, results from a few cases were selected for comparison in this report. These cases, exercises 3 and 4 (for profiles S – Simplified – and A - Actual) were chosen as they produced conditions of both no derailment and derailment, respectively.

- VII.1 CASE 1 - SIMPLIFIED “S” PROFILES

Wheel and rail “S” profiles were designed analytically (see Annex 1). The wheel tread is perfectly cylindrical without conicity or curvature while the rail top has a constant radius of 0.3m. The wheel flange is straight at 70° and the bottom has a constant radius.

The first flange contact occurs on this straight 70° section and on the rail shoulder that has a constant radius of 0.013 m. As a consequence, these first flanging impact conditions are simple and causes of differences in flanging forces could be analyzed easily. However, this first flanging contact is so close to the end of the straight flange section that further displacements can move the contact to the curved flange bottom.

The two point contact situation for the simplified “S” profiles is simple because both simultaneous contacts are elliptic.

- VII.1.1 Exercise 3S: initial lateral velocity = 1m/s

Complete comparisons are in the attached file [“ld_case1_ex3_simp_comp_nov06.pdf”](#)

The next two pages present comparisons of displacements and normal forces for a simulation time up to 100ms.

Displacements

Figure 1 shows the lateral, vertical, and roll displacements for exercise 3S provided from all seven participants. All three displacements of the six “type A” codes are quite similar. VAMPIRE lateral displacements are also similar. However, vertical and roll displacements still remain different.

Normal forces

Figure 2 shows the normal forces for exercise 3S provided from all seven participants. Normal forces of the six Hertzian codes are nearly identical. VAMPIRE normal forces BEYOND THE FIRST IMPACT are SIGNIFICANTLY different.

Considering normal forces of successive impacts, it was observed that VAMPIRE amplitudes, with the exception of the first impact, were different from the others. After the first impact, the tread normal force is suddenly and unexpectedly increasing over 1MN and negative forces appear at times. However, the VAMPIRE team observed that when the forces were quite high, the impulse width was reduced so that the impact on displacements was proper.

Questions were raised regarding the sudden reduction of lateral velocity that 5 of the codes calculate at the simulation time of 75ms to 90ms which could be an artifact while the stiff rebound of both the other codes looks more usual. This relates to the dynamics of impacts of a complex body against an inclined plane: when the wheelset impacts the rail, the total kinetic energy and momentum are conserved. The lateral evolution from impact depends on the lateral force magnitude that will be calculated (elastically or not) during impact. Assuming that all codes calculate approximately the same normal force direction, then there would be roughly three possible cases : - 1) the lateral component of the force is not large enough and the wheelset will continue to go right (possible derailment case) - 2) the lateral component of the force is such as to stop the lateral displacement (lateral velocity goes to zero); the energy is transferred to roll and vertical - 3) the lateral component of the force is large enough to reverse the lateral speed and the wheelset comes back.

Figure 3 shows the peak normal force at the first flange impact on the left wheel for exercise 3S. The peak normal force is nearly identical for all of the “type A” codes. Peak values were extracted from the data provided. Each code used different sample frequencies for their output data which may contribute to the differences in peak normal force. The output frequencies used by each of the codes for exercise 3S are shown in Table 1.

Table 1: Output Frequency for Exercise 3S.

DYNARAIL	7309 Hz
LDYN	20010 Hz
NUCARS	3288 Hz
SAMSRAIL	16675 Hz
SIMAPCK	5008 Hz
VAMPIRE	4010 Hz
VOCODYM+.4	10001 Hz

Federal Railroad Administration - VOLPE Center - French Ministry of Transportation

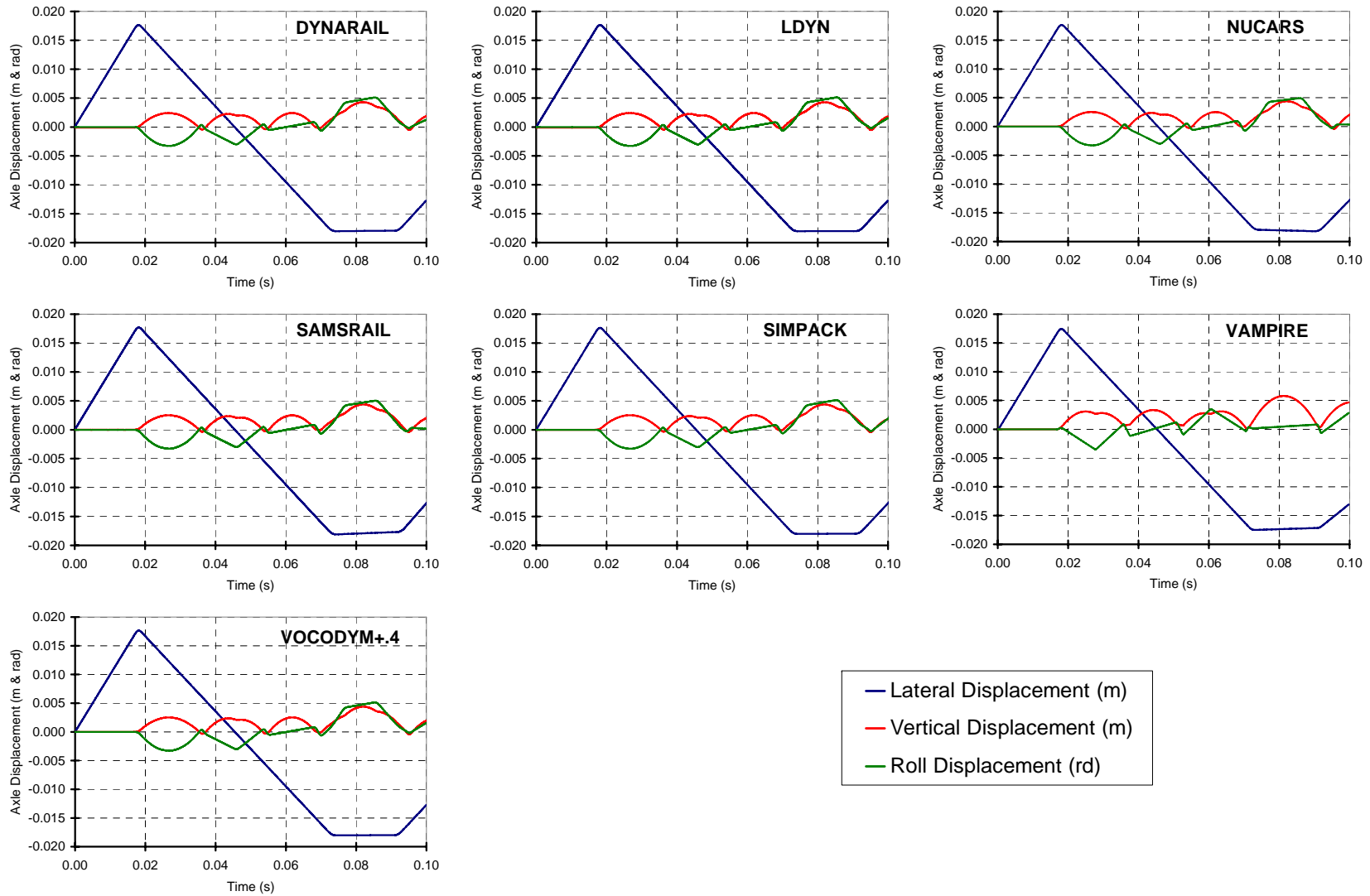


Figure 1: Displacements of Exercise 3S, initial lateral velocity = 1 m/s

Federal Railroad Administration - VOLPE Center - French Ministry of Transportation

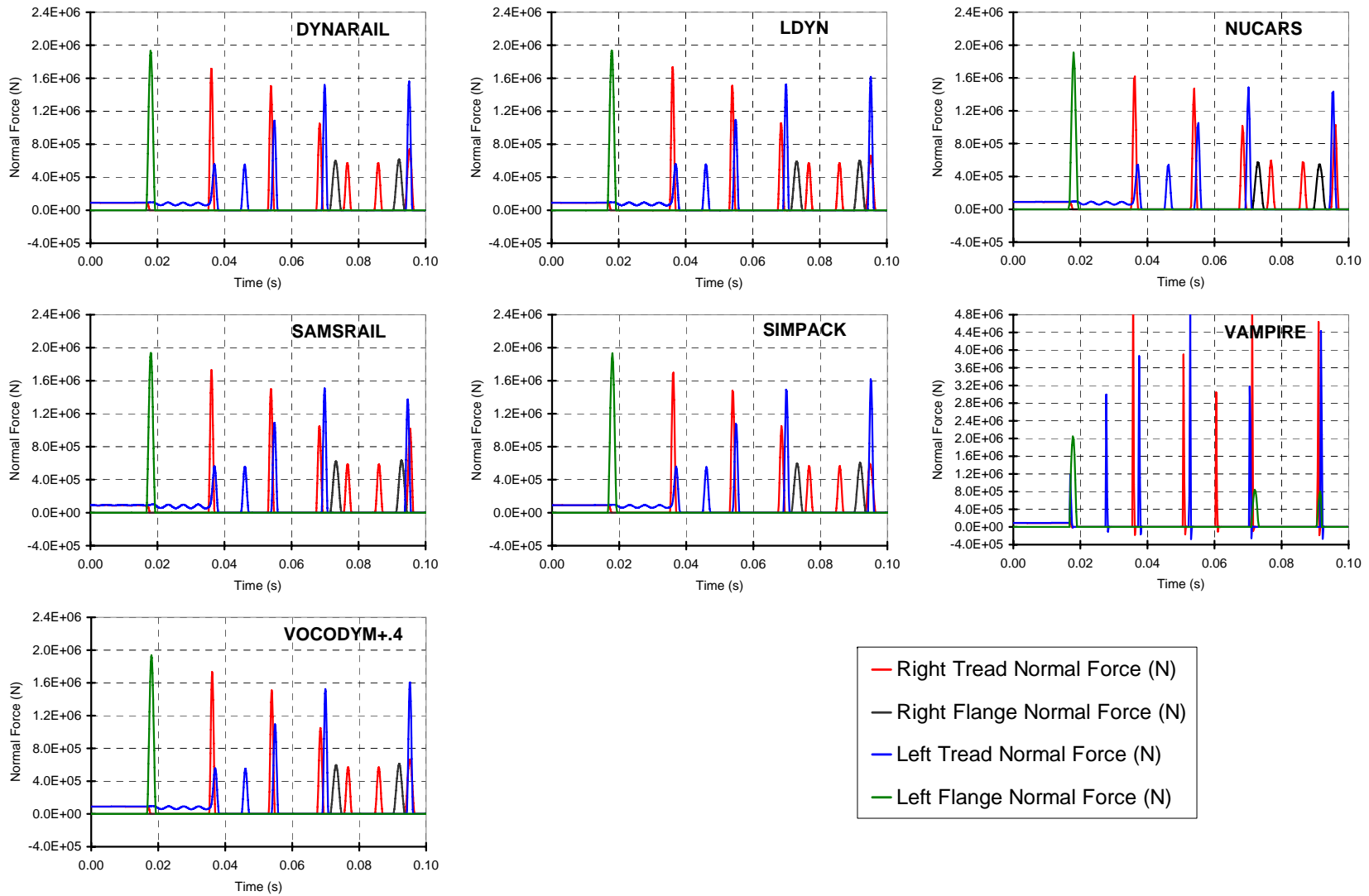


Figure 2: Normal Forces of Exercise 3S, initial lateral velocity = 1 m/s

Maximum Normal Force on Left Wheel Flange (First Impact)

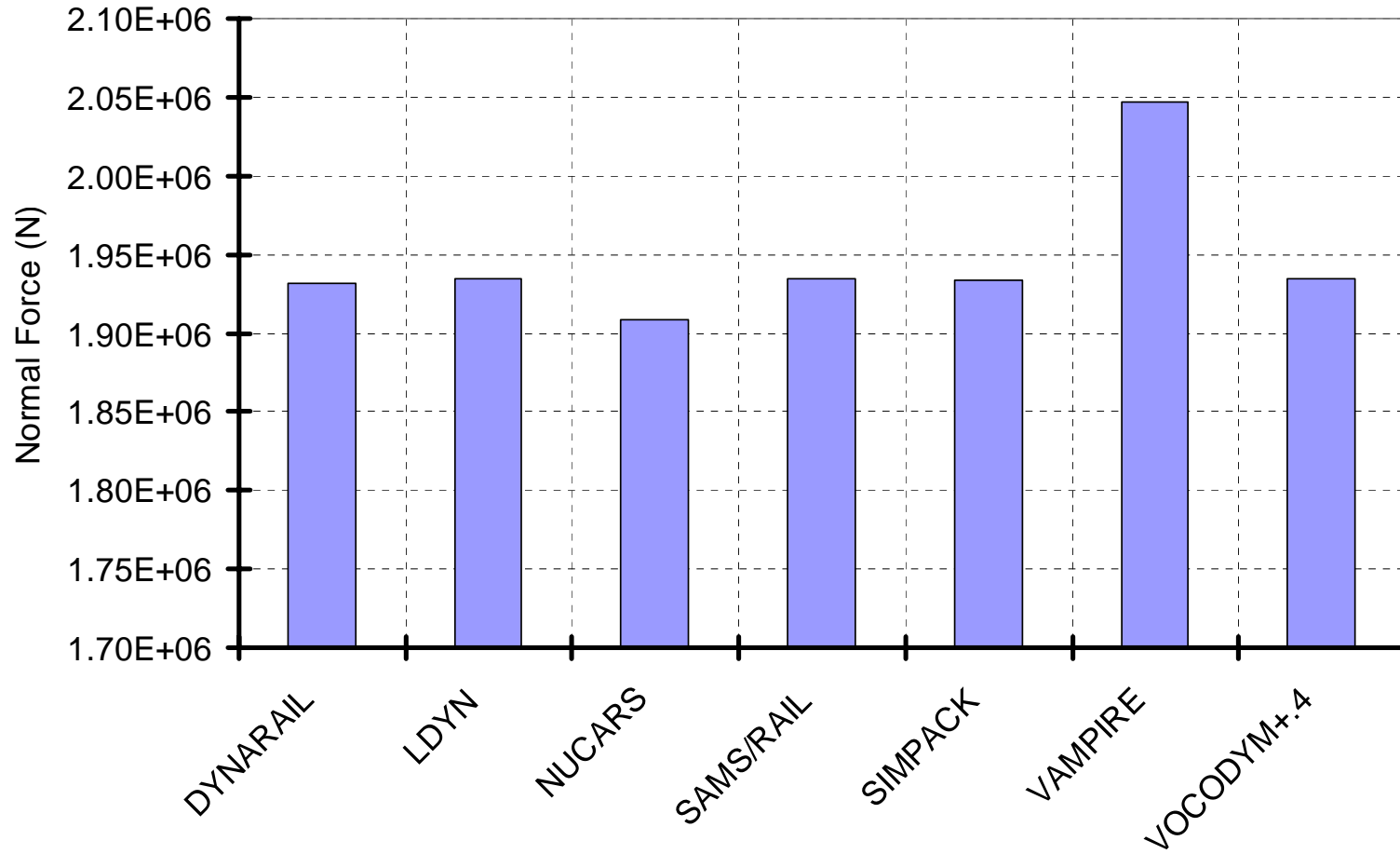


Figure 3: Peak Normal Forces of Exercise 3S at First Impact, initial lateral velocity = 1 m/s

- VII.1.2 Exercise 4S: initial lateral velocity = 2m/s

Complete comparisons are in the attached file "[ld_case1_ex4_simp_comp_nov06.pdf](#)"

The next two pages present comparisons of displacements and normal forces up to a simulation time of 200ms.

Displacements

Figure 4 shows the lateral, vertical, and roll displacements for exercise 4S provided from all seven participants. Displacements of the six "type A" codes are quite similar. VAMPIRE displacements are similar until at time of about 0.075 seconds, the time of the second impact on the left flange

Normal forces

Figure 5 shows the normal forces for exercise 4S provided from all seven participants. Normal forces of six "type A" codes are nearly identical. VAMPIRE normal forces are different.

Considering normal forces of successive impacts, it was observed that VAMPIRE amplitudes, with the exception of the first impact, were different from the others. After the first impact, the tread normal force is unexpectedly increasing over 1.5MN and negative forces appear at times down to 0.5MN. However, VAMPIRE team observed that when the forces were quite high, the impulse width was reduced so that the impact on displacements was proper.

Figure 6 shows the peak normal force at the first flange impact on the left wheel for exercise 4S. The peak normal force is nearly identical for all of the "type A" codes. Peak values were extracted from the data provided. Each code used different sample frequencies for their output data which may contribute to the differences in peak normal force. The output frequencies used by each of the codes for exercise 4S are shown in Table 2.

Table 2: Output Frequency for Exercise 4S.

DYNARAIL	3655 Hz
LDYN	20005 Hz
NUCARS	3283 Hz
SAMSRAIL	10005 Hz
SIMAPCK	5002 Hz
VAMPIRE	4010 Hz
VOCODYM+.4	10001 Hz

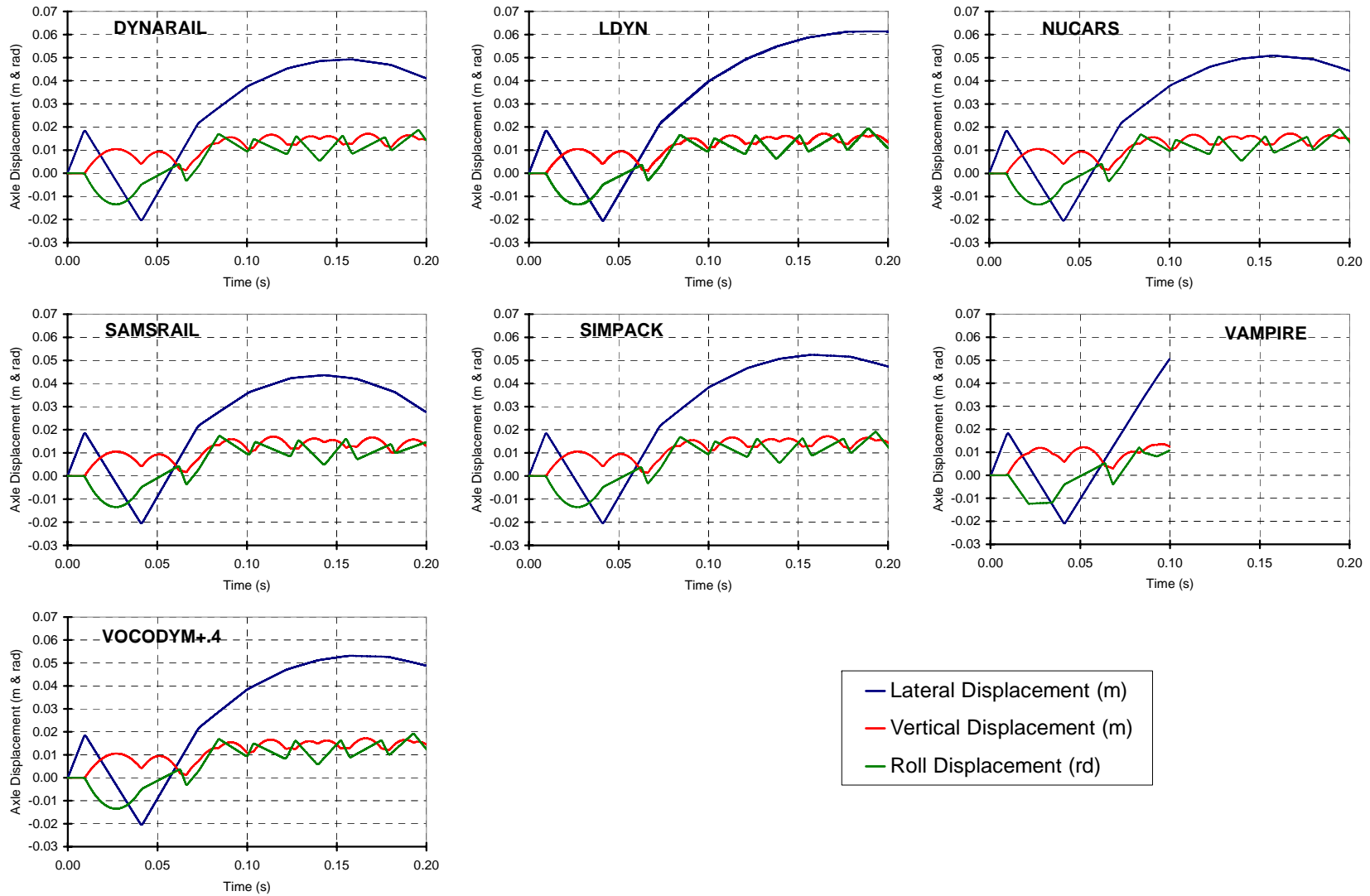


Figure 4: Displacements of Exercise 4S, initial lateral velocity = 2 m/s

Federal Railroad Administration - VOLPE Center - French Ministry of Transportation

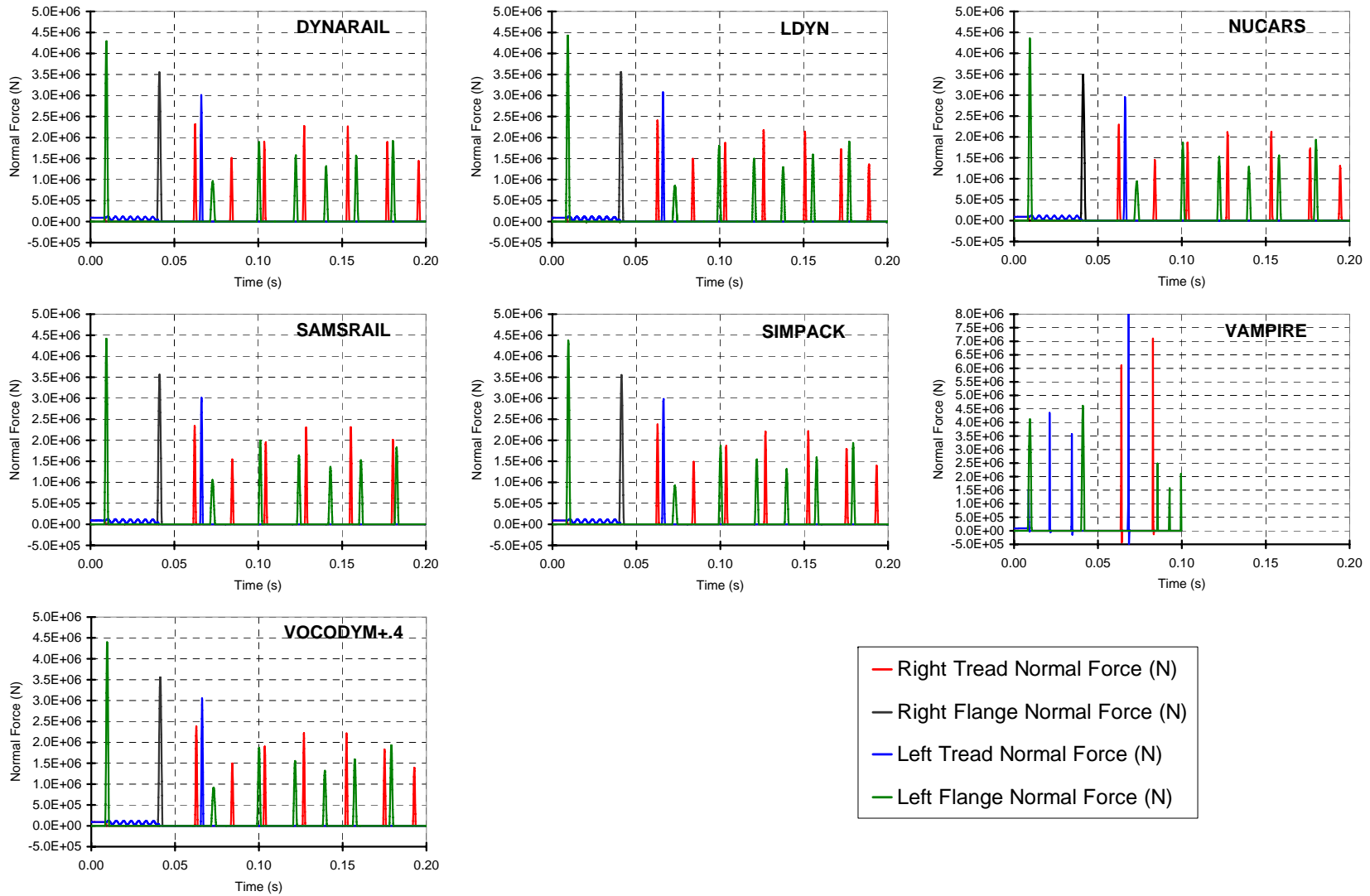


Figure 5: Normal Forces of Exercise 4S, initial lateral velocity = 2 m/s

Maximum Normal Force on Left Wheel Flange (First Impact)

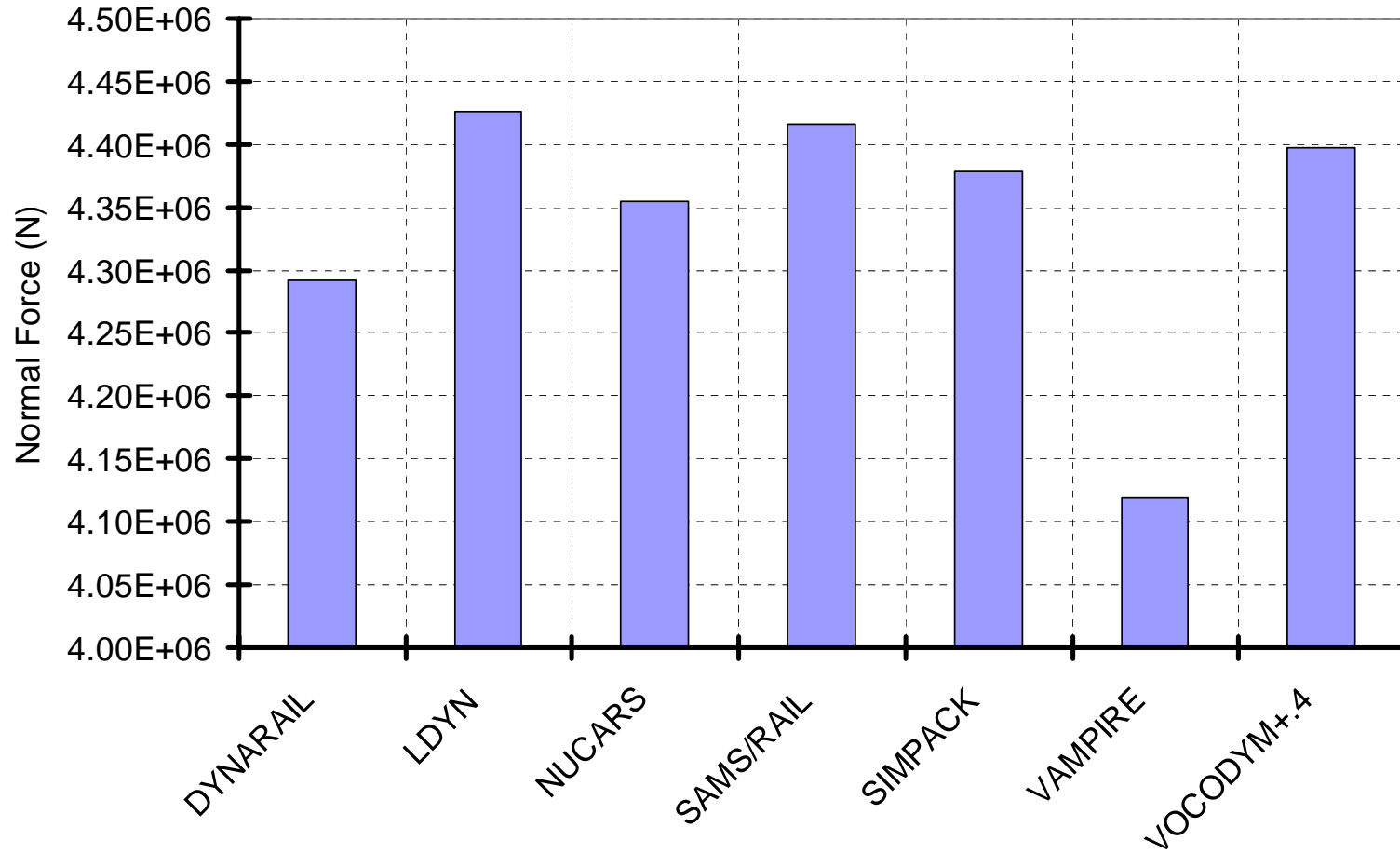


Figure 6: Peak Normal Forces of Exercise 4S at First Impact, initial lateral velocity = 2 m/s

- VII.2 CASE 1 - ACTUAL “A” PROFILES

Wheel and rail “A” profiles were designed numerically (see Annex 1). The wheel tread is tapered at 1/40 while the rail top has a constant radius of 0.254m (US140 rail). This wheel tread conicity induces a coupling between lateral and roll velocities in such a way that an initial roll velocity must be adjusted in order not to initiate oscillations.

The wheel shoulder and flange are curved. First flanging contact occurs at an area where wheel curvature and tangent are not constant, at an angle around 60° and at a point on the rail shoulder that has a relatively constant radius of about 0.0095 m. However, the contact point on the rail is not far from the straight, zero curvature, rail flange and it is necessary to verify that any profile smoothing does not modify significantly contact angles around this point.

As a consequence, this first flanging impact conditions, although not quite conforming, are not as simple as with simplified profiles and the causes of differences in flanging forces could not be analyzed easily.

It is thought that procedures that may have been used for smoothing these numerical profiles may have changed slightly the results and notably the functions tangents.

- VII.2.1 Exercise 3A: initial lateral velocity = 1m/s

Complete comparisons are in the attached file “[ld_case1_ex3_actual_comp_nov06.pdf](#)”

The next two pages present comparisons of displacements and normal forces up to 100ms.

Displacements

Figure 7 shows the lateral, vertical, and roll displacements for exercise 3A provided from all seven participants. Correlations between displacements of the six “type A” codes are clear only up to the second lateral impact, at 45 ms. After this time, correlations are unclear; however all lateral displacements after 100ms are close to each other. VAMPIRE vertical and roll displacements are different from the first impact.

Normal forces

Figure 8 shows the normal forces for exercise 3A provided from all seven participants. Normal forces of five of the six “type A” codes are similar.

NUCARS normal forces show a larger force at second impact (right side) and are missing the further right impact that are displayed by the other Hertzian codes. The missing second right impact explains differences in the shape of lateral displacement. Note that similar results were previously (June results) found by VOCODYM+ before using refined tables.

VAMPIRE normal forces are different. In addition large tread force oscillations with a tendency to increase are observed at the very beginning of the simulations and they disappear after the first impact. The VAMPIRE team explained that these oscillations are a consequence

of the specific way (impulse) that was used for setting initial lateral and roll velocities in VAMPIRE which normally cannot set initial velocities other than zero.

Figure 9 shows the peak normal force at the first flange impact on the left wheel for exercise 3A. The peak normal force is nearly identical for all of the “type A” codes. Peak values were extracted from the data provided. Each code used different sample frequencies for their output data which may contribute to the differences in peak normal force. The output frequencies used by each of the codes for exercise 3A are shown in Table 3.

Table 3: Output Frequency for Exercise 3A.

DYNARAIL	7309 Hz
LDYN	20010 Hz
NUCARS	3288 Hz
SAMSRAIL	10010 Hz
SIMAPCK	5011 Hz
VAMPIRE	4010 Hz
VOCODYM+.4	10001 Hz

Federal Railroad Administration - VOLPE Center - French Ministry of Transportation

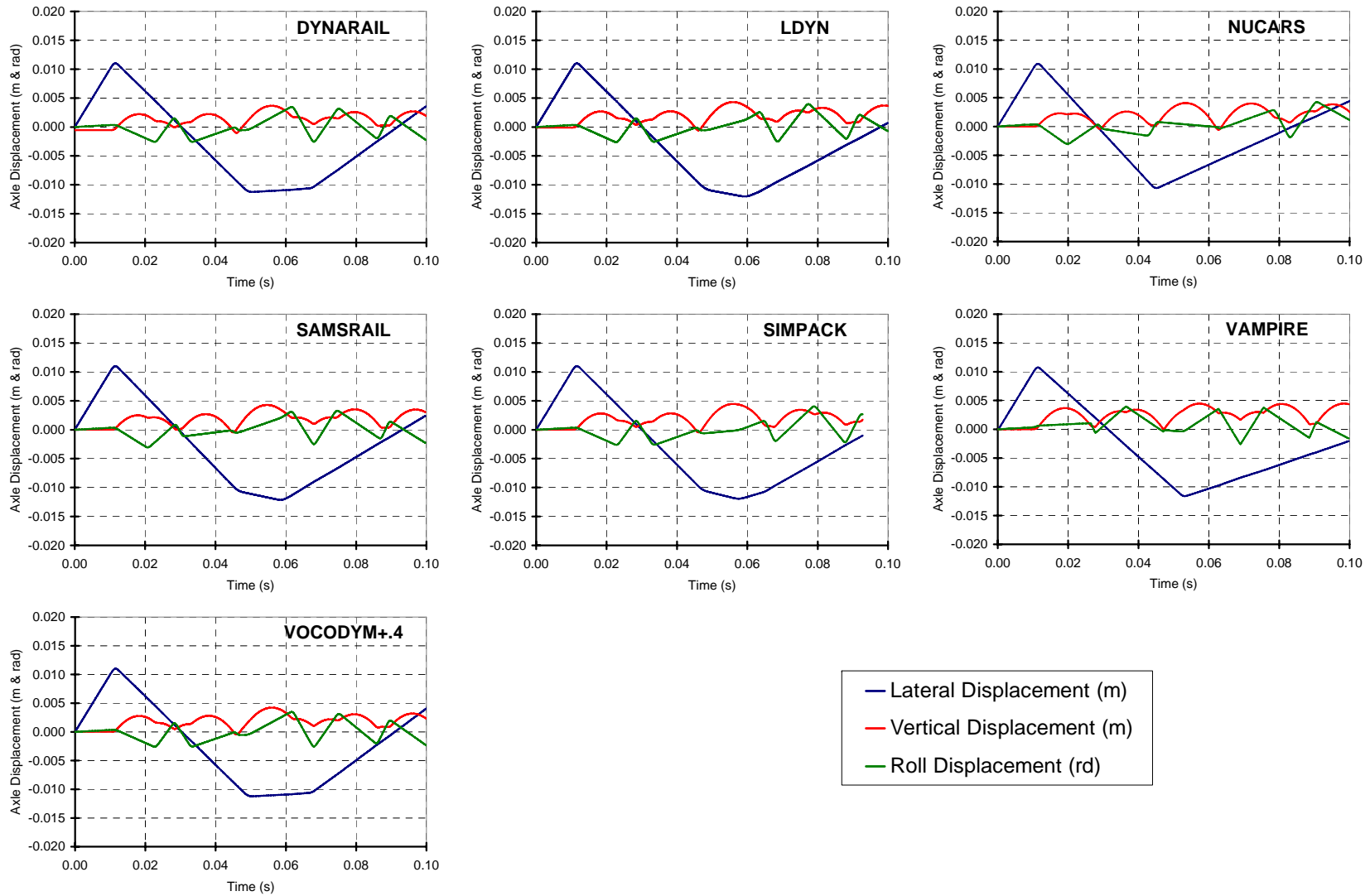


Figure 7: Displacements of Exercise 3A, initial lateral velocity = 1 m/s

Federal Railroad Administration - VOLPE Center - French Ministry of Transportation

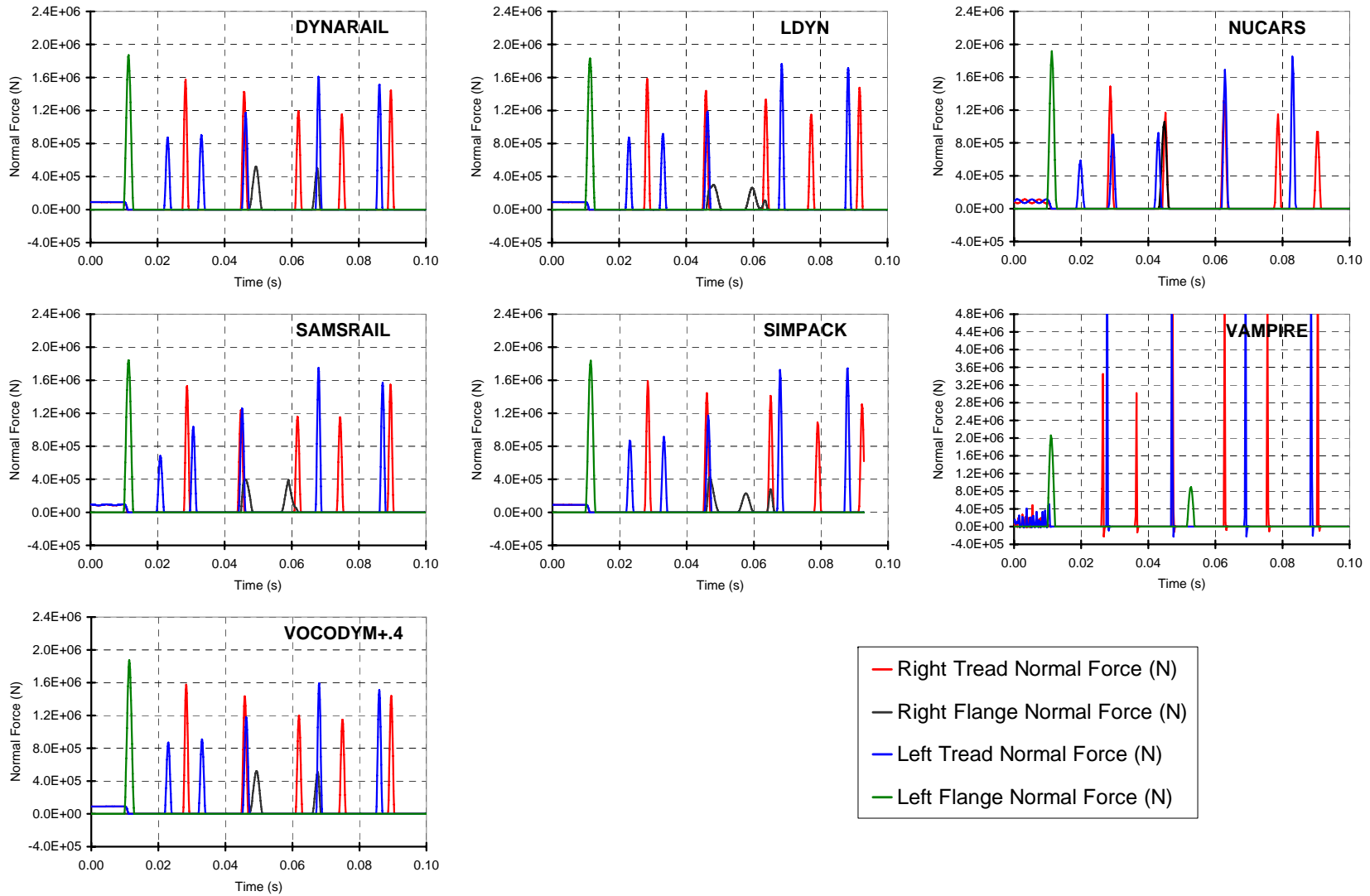


Figure 8: Normal Forces of Exercise 3A, initial lateral velocity = 1 m/s

Maximum Normal Force on Left Wheel Flange (First Impact)

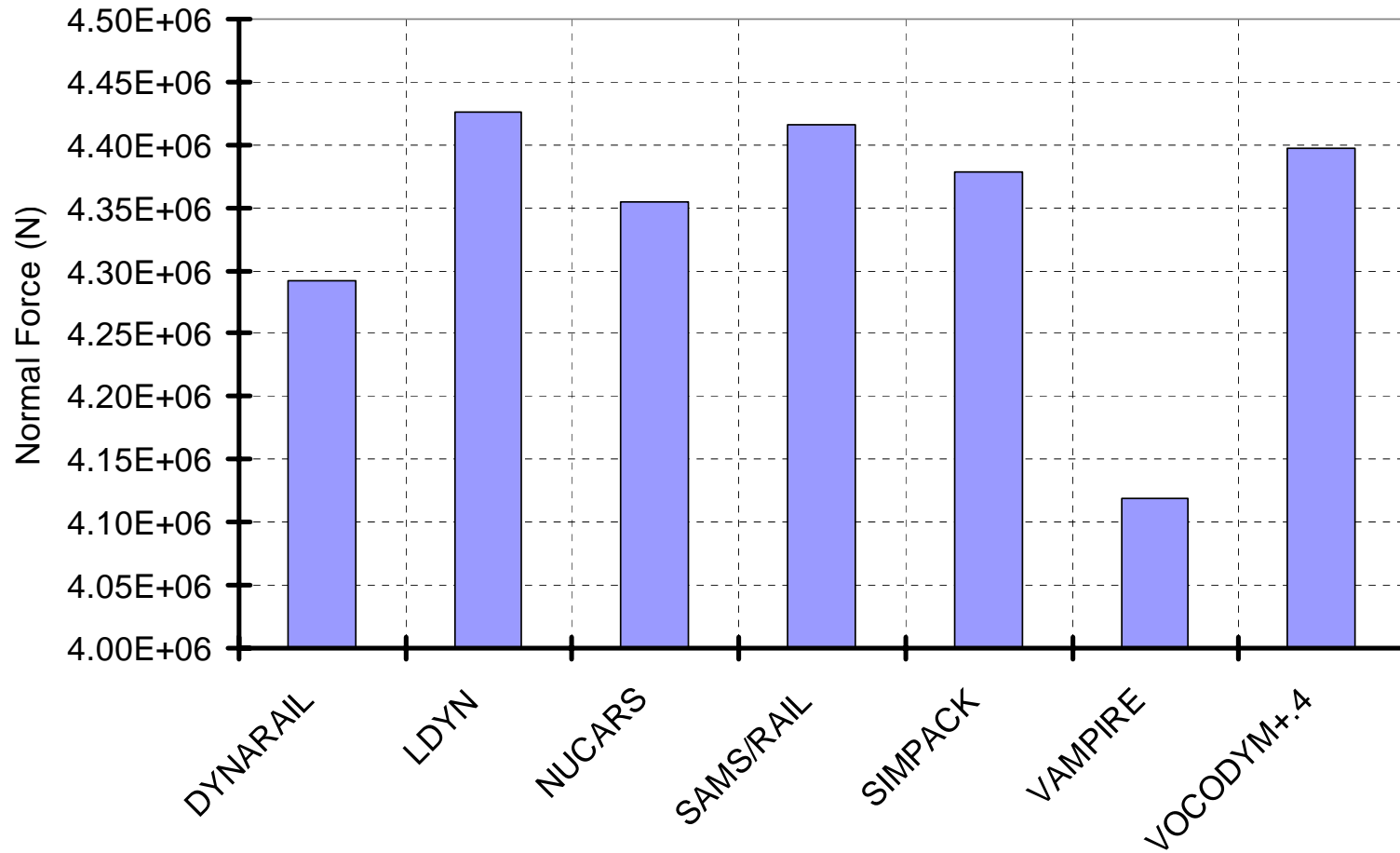


Figure 9: Peak Normal Forces of Exercise 3A at First Impact, initial lateral velocity = 1 m/s

- VII.2.2 Exercise 4A: initial lateral velocity = 2m/s

Complete comparisons are in the attached file "[ld_case1_ex4_actual_comp_nov06.pdf](#)"

The next two pages present comparisons of displacements and normal forces up to a simulation time of 100ms.

Displacements

Figure 10 shows the lateral, vertical, and roll displacements for exercise 4A provided from all seven participants. Correlations between displacements of five of the six "type A" codes are relatively clear. NUCARS is less correlated, however displacements are of same type. VAMPIRE (all 3 dof) displacements are very different after the first impact.

Normal forces

Figure 11 shows the normal forces for exercise 4A provided from all seven participants. Normal forces of five of the six "type A" codes are roughly similar. NUCARS forces progressively differ from the others in same proportion as in the previous exercise. VAMPIRE normal forces are different. In addition large tread force oscillations with a tendency to increase are observed at the very beginning of the simulations. The VAMPIRE team explained that these oscillations are a consequence of the specific way (impulse) that was used for setting initial lateral and roll velocities in VAMPIRE which normally cannot set initial velocities other than zero.

Figure 12 shows the peak normal force at the first flange impact on the left wheel for exercise 4A. The peak normal force is nearly the same all of the codes. Peak values were extracted from the data provided. Each code used different sample frequencies for their output data which may contribute to the differences in peak normal force. The output frequencies used by each of the codes for exercise 4A are shown in Table 4.

Table 4: Output Frequency for Exercise 4A.

DYNARAIL	7309 Hz
LDYN	20005 Hz
NUCARS	3282 Hz
SAMSRAIL	10010 Hz
SIMAPCK	5014 Hz
VAMPIRE	4010 Hz
VOCODYM+.4	10001 Hz

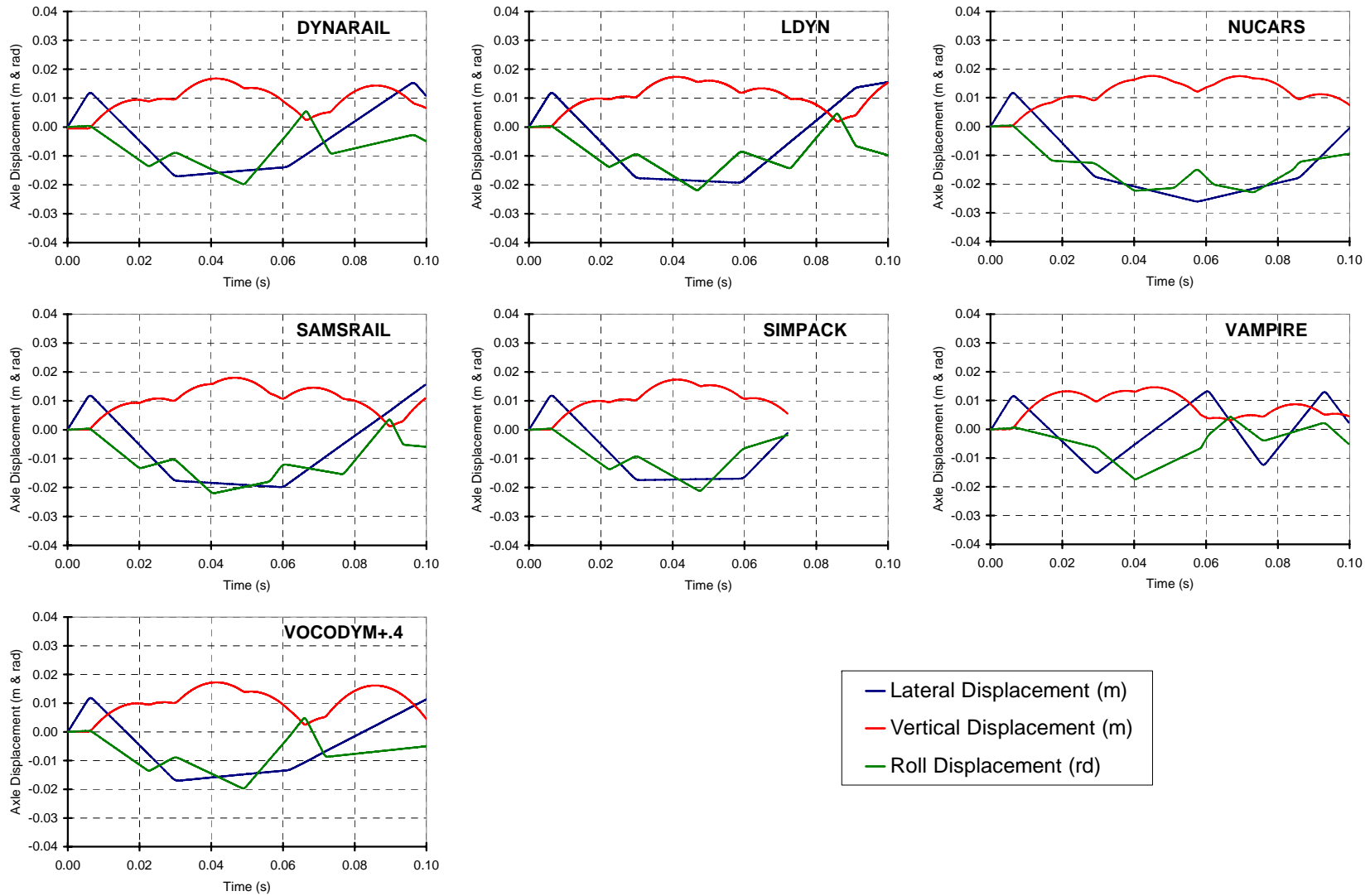


Figure 10: Displacements: Exercise 4A, initial lateral velocity = 2 m/s

Federal Railroad Administration - VOLPE Center - French Ministry of Transportation

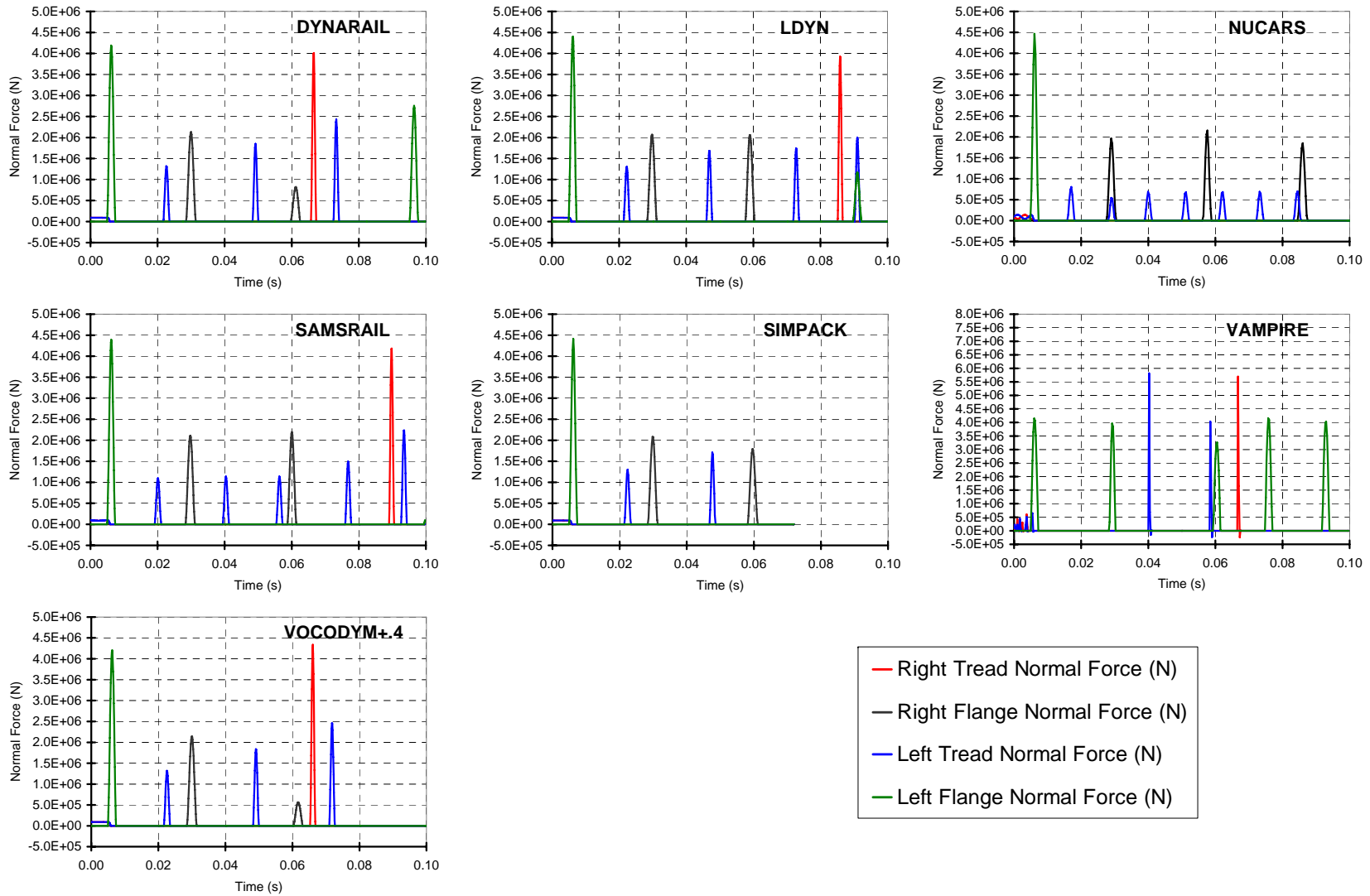


Figure 11: Normal Forces of Exercise 4A, initial lateral velocity = 2 m/s

Maximum Normal Force on Left Wheel Flange (First Impact)

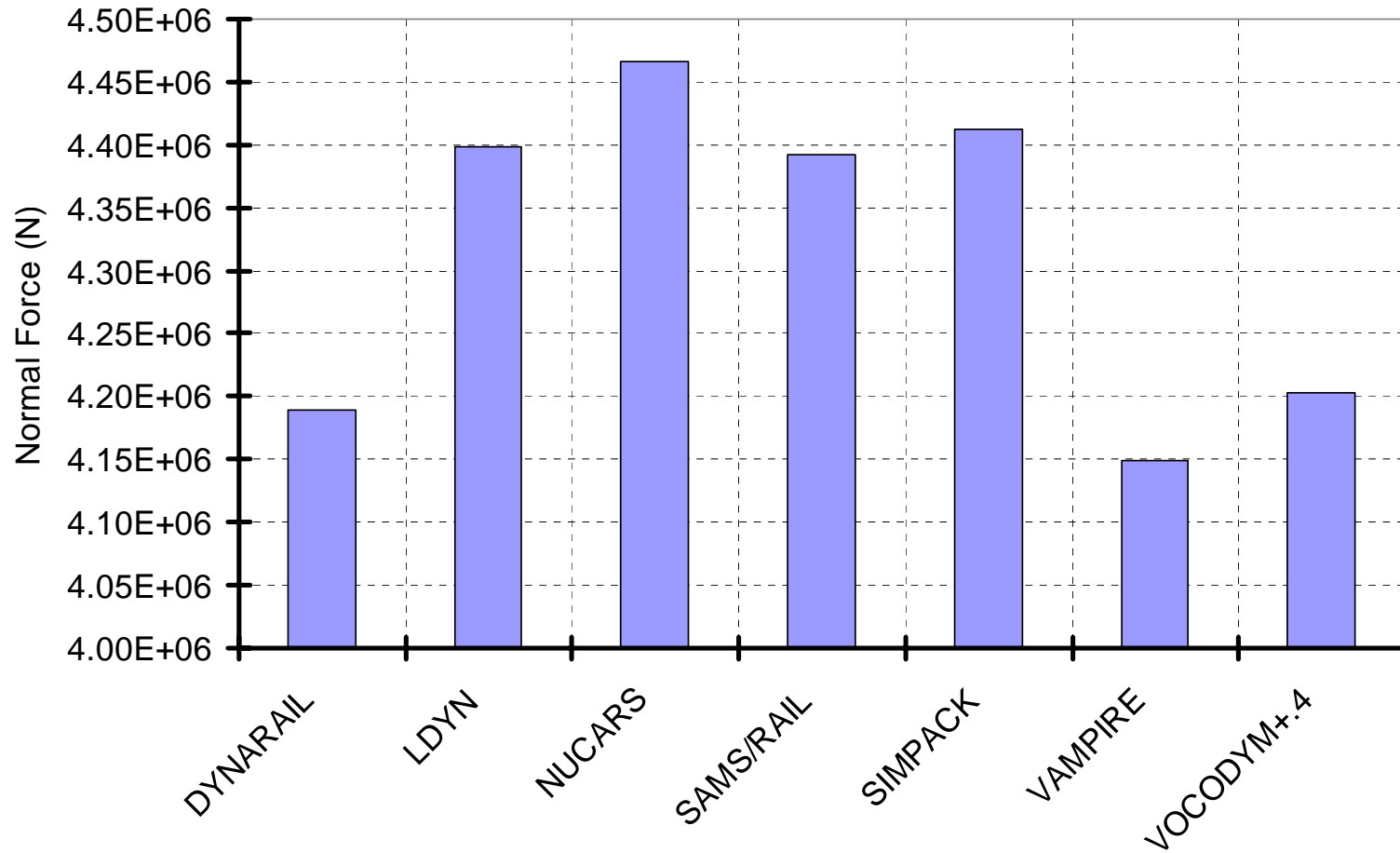


Figure 12: Peak Normal Forces of Exercise 4A at First Impact, initial lateral velocity = 2 m/s

- VIII - First Impact Details

Because significant differences appear in these results, it could be interesting to investigate further.

A first parameter found to be very sensitive was the track gage. This is easy to understand since it influences the time and the conditions of successive impacts. However, once the gage was carefully adjusted, differences still remained and attention was directed to the first impact itself.

Any small differences in calculation of this first impact, although not large, as seen at a global drawing scale, could lead to larger differences and different behaviors after some time. The main parameter influencing the rest of the simulation seems to be the contact angle. During lateral impacts, large normal forces develop for which the direction points more or less to the center of mass of the wheelset so that roll accelerations due to this normal flanging force are very sensitive to its direction. At some critical phases, small differences in the force direction (contact angle) can even change the sign of the roll acceleration.

Studying the results, it is clear that differences primarily begin with roll differences.

In order to understand these differences, and possibly eliminate other causes, it could be interesting to study the details of this first impact such as presented on the next page.

It was proposed to Participants who would like to compare similar results of first impact to add wheel and rail curvatures in their results and this could be the matter of a further extension to the Benchmark report if enough results would be available.

- IX - CONCLUSIONS

Notwithstanding that this benchmark problem was to focus only on calculation of normal contact forces, simulation results from one code did show appreciable differences.

Seven participants sent their results, each of them with different codes.

Of the three commercialised codes, NUCARS, SIMPACK, VAMPIRE , only VAMPIRE used a commercial version (VAMPIRE Pro). The other four codes used developmental beta versions at the time of benchmark closure (November 2006).

Six codes are using elastic wheel/rail contacts of the Hertzian type; the seventh code, VAMPIRE, uses a rigid contact with linear elasticity provided between the wheel and ground.

Six codes using Hertzian contact models have in principle the same hypotheses and their results show good correlations. Previous differences were found mainly in the use of interpolating pre-calculated tables of elliptic integrals and nearly disappeared using refined tables. However, although both profiles pairs were not at all of the conformal type, similarities between Hertzian results are better for the simplified profiles than for the actual profiles; larger differences are expected in the case of conformal profiles pairs and this leaves the field open to further improvements.

VAMPIRE showed appreciably different results. However, after adjusting the lateral wheel/ground stiffness, new displacements results of several cases are closer to results of Hertzian codes, including a derailment in the case with the largest initial lateral velocity, although the details of the derailment mechanism were not the same.

All simulation results of this case utilizing this highest initial lateral velocity showed severe derailment conditions by climbing over one rail as a consequence of a previous lateral impact on the other rail.

One main conclusion is a confirmation that, for wheelset behavior with flanging impacts, results are very sensitive to input parameters. Initial results also showed that track foundation stiffness also had a significant impact on prediction of wheel and rail contact forces. This strongly advocates in favor of developing parametric studies while assessing derailment risks.

Results suggest that codes using elastic contacts appear to be more consistent at predicting derailment resulting from the conditions in this benchmark. This may further suggest that these conditions may be more challenging to predict using rigid contact.

It is recommended to continue improving this benchmark by cooperating between researchers, notably in providing common results of Hertzian codes that could be published and used as confirmed targets in developing new softwares including new wheel/rail pairs with conformal situations.

Once this goal satisfied, harmonization of normal forces being calculated, it would be possible to further increase the complexity by adding track foundation models and wheel/rail friction in an extension of these exercises.

ANNEX 1 - BENCHMARK DATA - Call for Simulations: Dynamic Wheel/Rail Benchmark Single Wheelset without Friction

Benchmark Status

This problem is proposed by the FRA/DTT Cooperation Team to help analyze differences between several codes using either elastic normal calculations or constraint equations.

Even though reducing the model complexity to only one axle, analysis of its behavior would still be complex because mixing essential mechanisms: rolling, calculations of normal contact forces and dynamic equations. This very simple Benchmark (one single wheelset without friction, nor material damping between wheel and rail) is intended to analyze normal contact force calculations and modeling of flanging with impacts. Although one would believe it extremely elementary, it is expected to find different results due to differences in coding assumptions.

All interested parties are invited to participate in this benchmarking exercise and submit results no later than June 16, 2006. All submittals will be published in a joint FRA/DTT report in which all simulation results will compare with one another. The published report will be made available within 60 days of deadline.

LD BENCHMARK INPUT DATA

Wheelset

- Mass: 1568 kg
- Roll inertia: 656 kg.m²
- Pitch inertia¹: 168 kg.m²
- Rolling Radius: 0.457 m
- Wheels load at equilibrium: 90kN (wheelset is loaded with a vertical non inertial constant force of 164.618 kN – gravity: 9.81 m/s/s)
- 4 DOF: Lateral (Y), Vertical (Z), Roll (Φ), Pitch (Ω)
- Wheel Profiles: There are 2 wheel profiles in the non-linear exercises:
 - A. Actual wheel profile 1:40 taper “awprof” (numeric file: “awprof.yz”)
 - B. Simplified wheel profiles “swprof” (numeric file: “swprof.yz”)
 The files are provided in mm - See drawings page 5
- Back to Back spacing: 1.35214 m

Material Properties

- Poisson’s ratio = 0.28
- Modulus of elasticity 210000.0 N/mm²
- Modulus of rigidity 82000.0 N/mm²

Wheel-Rail Friction

- < 10⁻⁷ (as close to zero as possible without causing numerical problems)

Track

- Rails Profile: There are 2 rail profiles in the non-linear exercises:
 - A. Actual rail profile “arprof” (numeric file: “arprof.yz”)
 - B. Simplified rail profiles “srprof” (numeric file: “srprof.yz”)
 The files are provided in mm - See drawings page 5
 Data in numeric files include 1:40 cant.

¹ Pitch inertia and DOF are only necessary if the code takes gyroscopic effects into account (could be neglected)

ANNEX 1

- Gage: 1.4351 m (56.5") measured at 14mm below top of rails
- Suspension: rigid (or infinite mass)

BENCHMARKING EXERCISES

1st CASE : Wheelset is free with an initial lateral velocity

	Exercise 1	Exercise 2	Exercise 3	Exercise 4
Initial Conditions				
X	0	0	0	0
Y	0	0	0	0
Z	0	0	0	0
Pitch Ω	0	0	0	0
Roll Φ	0	0	0	0
dX/dt	1 m/s (constant)	1 m/s (constant)	1 m/s (constant)	1 m/s (constant)
dY/dt	0.1 m/s	0.5 m/s	1 m/s	2 m/s
dZ/dt	0	0	0	0
d Ω /dt	2.19 rad/s	2.19 rad/s	2.19 rad/s	2.19 rad/s
d Φ /dt	3.33 mrad/s	16.67 mrad/s	33.3 mrad/s	66.7 mrad/s
Constrained Degrees of Freedom				
Yaw	0 rad	0 rad	0 rad	0 rad

Note: roll velocity can also be internally linked to the imposed lateral velocity if the code uses rigid constraints.

In the 1st CASE, all participants are requested to carry out the 4 exercises twice: first using the data given above with a wheelset and rails having the actual wheel and rail profiles (awprof and arprof), and second using the data given above with a wheelset and rails having the simplified wheel and rail profiles (swprof and srprof).

Note: given the convention of Y positive to the left, the imposed lateral velocity will generate flange contact on the left wheel first. The simulation time for each exercise should be chosen such that the following sequence occurs: flange contact on the left wheel, flange contact on the right wheel, and the wheelset returns to center.

2nd CASE : Initial conditions: given in table below – a slowly growing lateral force (5.E3N/s) is applied at the wheelset CG up to derailment

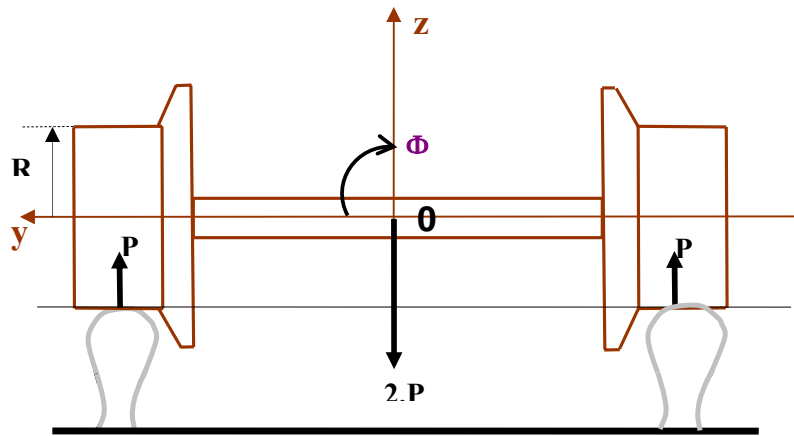
	Exercise 5
Initial Conditions	
X	0
Y	0
Z	0
Pitch Ω	0
Roll Φ	0
dX/dt	1 m/s (constant)
dY/dt	0
dZ/dt	0

ANNEX 1

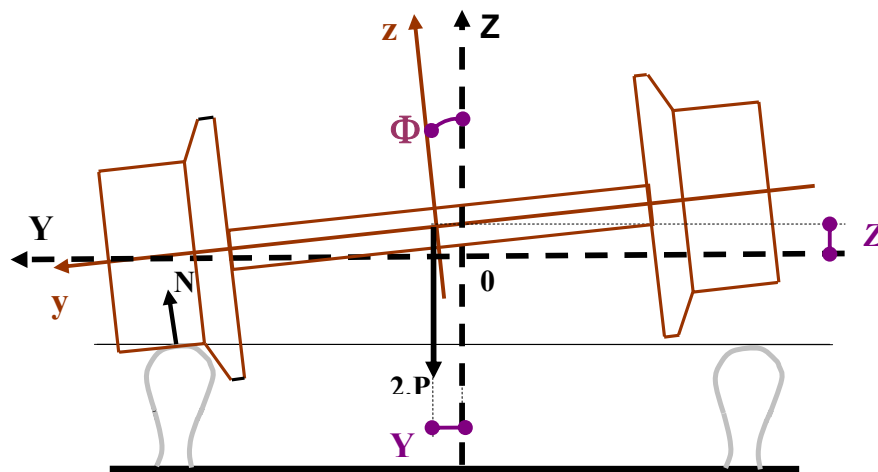
$d\Omega/dt$	2.19 rad/s
$d\Phi/dt$	0
Constrained Degrees of Freedom	
Yaw	0 rad

In the 2nd CASE, all participants are requested to carry out the exercise 5 twice: first using the data given above with a wheelset and rails having the actual wheel and rail profiles (awprof and arprof), and second using the data given above with a wheelset and rails having the simplified wheel and rail profiles (swprof and srprof).

Note: the external force applied at the CG should be oriented in the lateral direction defined by the track coordinate system. As the wheelset moves to the left, the wheelset will roll and the wheelset coordinate system will no longer coincide with the track coordinate system as shown in the figures below. The simulation time for each exercise should be sufficient to allow for wheelset derailment.



Coordinate System Convention



Typical Wheelset Roll Relative to Track [Y, Z, Φ]

SIMULATIONS AND REPORTING OF RESULTS

Frame: Y positive to the left, Z positive upwards

Plots as functions of time in track frame:

Wheelset Lateral Displacement Y

Wheelset Vertical Displacement Z

Wheelset Roll Displacement Φ

Wheelset Lateral Velocity

Wheelset Vertical Velocity

Wheelset Roll Velocity

Wheelset Lateral Acceleration

Wheelset Vertical Acceleration

Wheelset Roll Acceleration

Contact angles on tread and flange of both left and right wheels

Normal forces on tread and flange of both left and right wheels

Vertical forces on tread and flange of both left and right wheels

Lateral forces on tread and flange of both left and right wheels

Position of every contact point (lateral and vertical location)

Rolling radius at every contact point

Energy balance (kinetic and potential energy components)

Numerical files of profiles are available at the VOLPE Center Site:

<ftp://ftp.volpe.dot.gov/pub/dts76/marquis/ldbenchmark/>

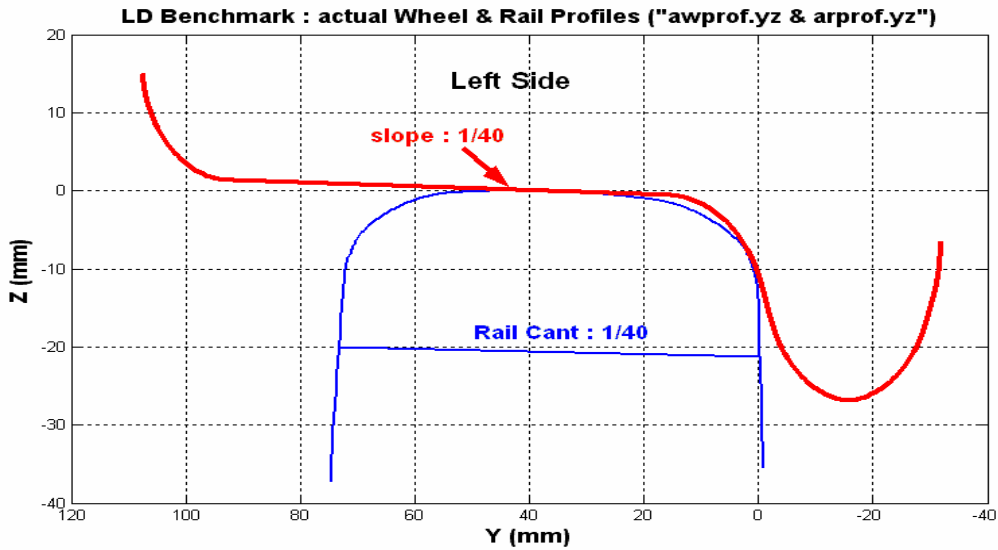
Simulation results should be sent either to Brian Marquis or to Jean-Pierre Pascal:

Brian.Marquis@volpe.dot.gov

pascal.voc@wanadoo.fr

who will publish the responses on the Volpe Center site in June 2006. Requested results should be submitted in 2 file formats. The first group of files should be an ASCII file for each simulation containing time histories results in labeled columns (5 exercises x 2 wheel/rail combinations = 10 ASCII files total). The output frequency should be sufficient to accurately capture all dynamic behavior. The second file should be a pdf file containing plots of each result. This will provide a means of verifying our understanding of the ASCII files. Along with the results, the organizers request each participant submit a brief abstract (maximum 4 pages) describing the program used and details of the wheel/rail contact force algorithm.

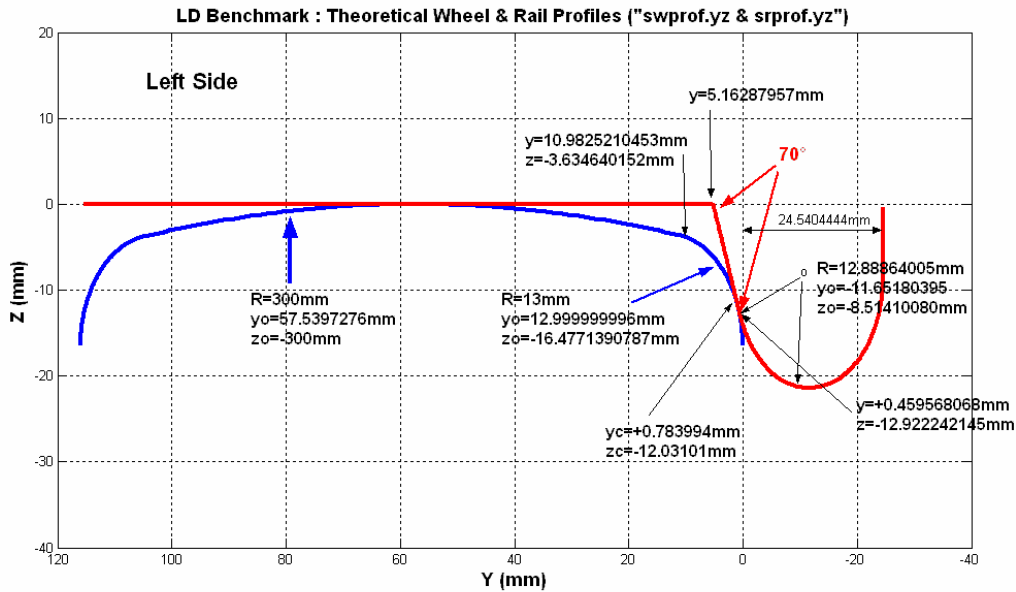
Wheel and Rail Profiles



Actual Wheel and Rail Profiles (numeric files)

note: in the numeric file, wheel back is at $y=0$ (shifted in the drawing)
and rail gage point is also at $y=0$ (not shifted)

Using benchmark data, rigid axle clearance results at $2 \times 10.18\text{mm}$



Theoretical Wheel and Rail Profiles (also in numeric files)

note: in the numeric file, wheel back is at $y=0$ (shifted by 24.54mm in the drawing)
and rail vertical is at $y=0$ (not shifted)

Using benchmark data, rigid axle clearance results at $2 \times 16.94\text{mm}$

ANNEX 2 - CODES STATUS -

LD Benchmark Participants

Code Version and Availability as of Benchmark Deadline (June 16, 2006)

DYNARAIL

DynaRail Version 2.06 has been developed by Jalil R. Sany jrsany@ameritech.net at CAM, Center for Automated Mechanics, USA. This program is the property of CAM and it will be commercially available before January 2007. The Hertzian elastic wheel/rail contact which has been used to simulate these benchmark problems will be the standard contact model in the upcoming released version.

LDYN

LDYN Beta Version was developed by and is solely available to Montpellier University, France

NUCARS

NUCARS® Version 2006 was developed by and is the property of Transportation Technology Center, Inc. USA. It is commercially available. The wheel/rail penetration algorithm used in the benchmark study is now available for use by all licensed users starting in September 2006. The option of using infinite rail support stiffness will be released in the next version. NUCARS® is a registered trademark of Transportation Technology Center, Inc. Further information is available at <http://www.ttc.aar.com/nucars/>

SAMSRAIL

SAMSRAIL is developed under a joint program between the Federal Railroad Administration (FRA) and University of Illinois at Chicago (UIC). It is currently available to FRA in beta version.

SIMPACK

SIMPACK was originally developed by the DLR (German aerospace research center) and MAN Technologie AG. INTEC GmbH, in Wessling Germany, is responsible for the development, marketing and sales of SIMPACK. SIMPACK and the module SIMPACK Wheel/Rail are commercially available and are used by manufacturers, operators and consultants all over the world. SIMPACK version 8.804 was used for the benchmark, which includes SIMPACK's redesigned wheel/rail contact. This is currently available as a beta version for interested customers.

VAMPIRE

VAMPIRE Pro Version 5.00 is developed by DELTARAIL (formerly AEAT). This product is commercially available. It is currently used worldwide by train manufacturers, train operators, infrastructure companies, railway authorities, consultancies and universities.

VOCODYM+

VOCODYM was developed by INRETS-SNCF. Contact Model of VOCODYM+ was developed by and is solely available to Dr. Jean-Pierre Pascal, France.

ANNEX 3 - HERTZ FORMULA -

Elastic Hertzian Calculations allow the calculation of elliptical contact patch dimensions and body's indentation as functions of applied load and body's main curvatures. These calculations require a numerical calculation of at least 3 elliptic integrals: B, E and K.

Before the age of computers, it was usual to rely on tabulated results for elliptic integrals as functions of a geometric parameter, γ , or tables of intermediate coefficients m, n, r as functions of geometric parameter θ . Although it is now easy to compute elliptic integrals online, it remains usual to rely on tables. If accurate results are requested, refined tables are necessary (see Annex 4).

Following Hertz equations can take different shapes:

Material Properties

- $E = 2.1000 \text{ E11 N/m}^2$
- $G = 8.2031 \text{ E10 N/m}^2$
- $\nu = 0.28$
- $Q = (1-\nu)/G$

Geometry

- RWX, RWY = Wheel longitudinal and transverse radius of curvature
- RRX, RRY = Rail longitudinal and transverse radius of curvature
- $D1 = (1/RWY + 1/RRY)/2$
- $D2 = (1/RWX + 1/RRX)/2$
- $\Delta = D1 + D2$

Elliptic Integrals

- $g = \text{ratio of ellipse axes } (g < 1)$
- $k^2 = 1 - g^2$
- $E = \int_0^{\pi/2} \{1 - k^2 \cdot \sin^2(\phi)\}^{1/2} d\phi$
- $K = \int_0^{\pi/2} \{1 - k^2 \cdot \sin^2(\phi)\}^{-1/2} d\phi$
- $B = (E - K \cdot g^2) / k^2$

Geometric Coefficients (input to tables)

- $\gamma = D1/\Delta = B/E$
- or
- $\cos\theta = (D1 - D2) / \Delta = (2B - E) / E$

Hertz Tabulated Coefficients (as a function of θ)

$$m = \left(\frac{2E}{\pi g^2} \right)^{1/3}$$

$$n = \left(\frac{2Eg}{\pi} \right)^{1/3}$$

$$r = \frac{K}{E^{1/3}} \left(\frac{2g}{\pi} \right)^{2/3}$$

$$g = n/m$$

Ellipse Parameters for 1N load

$$\underline{\delta} = r \left(\frac{9\Delta Q^2}{16} \right)^{1/3} \quad (\text{indentation for } F=1\text{N})$$

$$\underline{a} = m \left(\frac{3Q}{4\Delta} \right)^{1/3} \quad (\text{large semi-axis for } F=1\text{N})$$

$$\underline{b} = n \left(\frac{3Q}{4\Delta} \right)^{1/3} \quad (\text{small semi-axis for } F=1\text{N})$$

or

$$\underline{\delta} = \frac{K \underline{b}^2 \Delta}{E} \quad (\text{Kalker's shape})$$

$$\underline{b} = \left(\frac{3EgQ}{2\pi\Delta} \right)^{1/3} \quad (\text{Kalker's shape})$$

$$\underline{a} = \underline{b}/g \quad (\text{Kalker's shape})$$

With a load F

$$\delta = F^{2/3} \underline{\delta} = F^{2/3} r \left(\frac{9\Delta Q^2}{16} \right)^{1/3}$$

$$F = \delta^{3/2} / \underline{\delta}^{3/2} = \delta^{3/2} K_h$$

$$K_h = \underline{\delta}^{-3/2}$$

$$a = F^{1/3} \underline{a} = m \left(\frac{3FQ}{4\Delta} \right)^{1/3}$$

$$b = F^{1/3} \underline{b} = n \left(\frac{3FQ}{4\Delta} \right)^{1/3}$$

**ANNEX 4 – ELLIPTIC
INTEGRALS REFINED TABLES**

(J.P. Pascal)

$\theta(d^\circ)$	m	n	r	θ	m	n	r
1	37.32630	0.13105	0.12084	47	1.85371	0.61851	0.86809
2	22.29199	0.16913	0.17923	48	1.81932	0.62588	0.87449
3	16.48153	0.19659	0.22466	49	1.78616	0.63327	0.88071
4	13.29865	0.21890	0.26304	50	1.75415	0.64069	0.88674
5	11.23996	0.23813	0.29688	51	1.72323	0.64813	0.89259
6	9.78878	0.25522	0.32739	52	1.69336	0.65562	0.89827
7	8.70349	0.27074	0.35532	53	1.66446	0.66314	0.90377
8	7.85664	0.28506	0.38117	54	1.63649	0.67070	0.90910
9	7.17453	0.29841	0.40532	55	1.60941	0.67830	0.91426
10	6.61151	0.31098	0.42801	56	1.58317	0.68596	0.91925
11	6.13862	0.32289	0.44944	57	1.55773	0.69366	0.92408
12	5.73437	0.33425	0.46977	58	1.53305	0.70141	0.92874
13	5.38444	0.34513	0.48912	59	1.50909	0.70923	0.93325
14	5.07822	0.35560	0.50759	60	1.48582	0.71710	0.93759
15	4.80772	0.36571	0.52526	61	1.46322	0.72504	0.94178
16	4.56675	0.37550	0.54221	62	1.44124	0.73304	0.94581
17	4.35052	0.38501	0.55849	63	1.41987	0.74112	0.94969
18	4.15521	0.39427	0.57417	64	1.39907	0.74926	0.95342
19	3.97790	0.40331	0.58927	65	1.37883	0.75749	0.95699
20	3.81601	0.41215	0.60384	66	1.35911	0.76580	0.96042
21	3.66764	0.42081	0.61792	67	1.33989	0.77419	0.96369
22	3.53103	0.42930	0.63153	68	1.32116	0.78267	0.96682
23	3.40478	0.43765	0.64470	69	1.30289	0.79124	0.96980
24	3.28772	0.44587	0.65745	70	1.28507	0.79990	0.97264
25	3.17883	0.45397	0.66981	71	1.26768	0.80867	0.97533
26	3.07726	0.46196	0.68179	72	1.25069	0.81754	0.97788
27	2.98227	0.46986	0.69342	73	1.23410	0.82652	0.98029
28	2.89319	0.47767	0.70471	74	1.21789	0.83560	0.98256
29	2.80949	0.48540	0.71566	75	1.20204	0.84481	0.98468
30	2.73066	0.49306	0.72631	76	1.18655	0.85413	0.98667
31	2.65627	0.50066	0.73665	77	1.17139	0.86358	0.98851
32	2.58594	0.50820	0.74670	78	1.15656	0.87316	0.99022
33	2.51934	0.51570	0.75647	79	1.14204	0.88287	0.99178
34	2.45616	0.52315	0.76598	80	1.12782	0.89272	0.99321
35	2.39614	0.53057	0.77521	81	1.11389	0.90271	0.99451
36	2.33903	0.53795	0.78420	82	1.10024	0.91285	0.99566
37	2.28462	0.54531	0.79293	83	1.08686	0.92315	0.99668
38	2.23271	0.55265	0.80143	84	1.07374	0.93360	0.99756
39	2.18313	0.55998	0.80970	85	1.06087	0.94422	0.99831
40	2.13571	0.56729	0.81774	86	1.04825	0.95501	0.99892
41	2.09032	0.57459	0.82555	87	1.03585	0.96598	0.99939
42	2.04681	0.58190	0.83315	88	1.02369	0.97713	0.99973
43	2.00507	0.58920	0.84055	89	1.01174	0.98846	0.99993
44	1.96499	0.59651	0.84773	90	1	1	1
45	1.92646	0.60383	0.85471				
46	1.88940	0.61116	0.86150				

ANNEX 4

γ	g	E	K
5.00000e -001	1.00000e +000	1.57080e +000	1.57080e +000
5.03770e -001	9.90000e -001	1.56295e +000	1.57870e +000
5.07580e -001	9.80000e -001	1.55513e +000	1.58670e +000
5.11420e -001	9.70000e -001	1.54732e +000	1.59481e +000
5.15300e -001	9.60000e -001	1.53954e +000	1.60302e +000
5.19230e -001	9.50000e -001	1.53178e +000	1.61134e +000
5.23190e -001	9.40000e -001	1.52404e +000	1.61977e +000
5.27190e -001	9.30000e -001	1.51632e +000	1.62830e +000
5.31230e -001	9.20000e -001	1.50862e +000	1.63696e +000
5.35310e -001	9.10000e -001	1.50094e +000	1.64573e +000
5.39430e -001	9.00000e -001	1.49329e +000	1.65462e +000
5.43600e -001	8.90000e -001	1.48566e +000	1.66363e +000
5.47800e -001	8.80000e -001	1.47805e +000	1.67277e +000
5.52040e -001	8.70000e -001	1.47047e +000	1.68203e +000
5.56330e -001	8.60000e -001	1.46291e +000	1.69143e +000
5.60660e -001	8.50000e -001	1.45538e +000	1.70096e +000
5.65030e -001	8.40000e -001	1.44787e +000	1.71063e +000
5.69450e -001	8.30000e -001	1.44038e +000	1.72044e +000
5.73900e -001	8.20000e -001	1.43292e +000	1.73039e +000
5.78400e -001	8.10000e -001	1.42549e +000	1.74050e +000
5.82950e -001	8.00000e -001	1.41808e +000	1.75075e +000
5.87540e -001	7.90000e -001	1.41070e +000	1.76117e +000
5.92170e -001	7.80000e -001	1.40335e +000	1.77174e +000
5.96840e -001	7.70000e -001	1.39603e +000	1.78248e +000
6.01560e -001	7.60000e -001	1.38873e +000	1.79338e +000
6.06330e -001	7.50000e -001	1.38147e +000	1.80446e +000
6.11130e -001	7.40000e -001	1.37423e +000	1.81572e +000
6.15990e -001	7.30000e -001	1.36703e +000	1.82716e +000
6.20890e -001	7.20000e -001	1.35985e +000	1.83879e +000
6.25830e -001	7.10000e -001	1.35271e +000	1.85062e +000
6.30820e -001	7.00000e -001	1.34559e +000	1.86264e +000
6.35850e -001	6.90000e -001	1.33851e +000	1.87487e +000
6.40930e -001	6.80000e -001	1.33146e +000	1.88731e +000
6.46050e -001	6.70000e -001	1.32445e +000	1.89997e +000
6.51210e -001	6.60000e -001	1.31747e +000	1.91286e +000
6.56430e -001	6.50000e -001	1.31053e +000	1.92597e +000
6.61680e -001	6.40000e -001	1.30362e +000	1.93933e +000
6.66980e -001	6.30000e -001	1.29674e +000	1.95293e +000
6.72330e -001	6.20000e -001	1.28991e +000	1.96679e +000
6.77720e -001	6.10000e -001	1.28311e +000	1.98091e +000
6.83150e -001	6.00000e -001	1.27635e +000	1.99530e +000
6.88630e -001	5.90000e -001	1.26963e +000	2.00998e +000
6.94150e -001	5.80000e -001	1.26295e +000	2.02494e +000
6.99710e -001	5.70000e -001	1.25631e +000	2.04021e +000
7.05310e -001	5.60000e -001	1.24971e +000	2.05579e +000
7.10950e -001	5.50000e -001	1.24316e +000	2.07169e +000
7.16640e -001	5.40000e -001	1.23665e +000	2.08793e +000
7.22360e -001	5.30000e -001	1.23018e +000	2.10452e +000
7.28130e -001	5.20000e -001	1.22376e +000	2.12147e +000
7.33930e -001	5.10000e -001	1.21738e +000	2.13880e +000
7.39770e -001	5.00000e -001	1.21106e +000	2.15652e +000
7.45650e -001	4.90000e -001	1.20478e +000	2.17464e +000
7.51560e -001	4.80000e -001	1.19855e +000	2.19319e +000

ANNEX 4

γ	g	E	K
7.57500e -001	4.70000e -001	1.19237e +000	2.21218e +000
7.63480e -001	4.60000e -001	1.18624e +000	2.23163e +000
7.69490e -001	4.50000e -001	1.18017e +000	2.25156e +000
7.75520e -001	4.40000e -001	1.17415e +000	2.27200e +000
7.81590e -001	4.30000e -001	1.16819e +000	2.29296e +000
7.87680e -001	4.20000e -001	1.16229e +000	2.31447e +000
7.93790e -001	4.10000e -001	1.15644e +000	2.33657e +000
7.99930e -001	4.00000e -001	1.15066e +000	2.35926e +000
8.06090e -001	3.90000e -001	1.14493e +000	2.38260e +000
8.12260e -001	3.80000e -001	1.13927e +000	2.40660e +000
8.18440e -001	3.70000e -001	1.13367e +000	2.43132e +000
8.24640e -001	3.60000e -001	1.12815e +000	2.45677e +000
8.30850e -001	3.50000e -001	1.12268e +000	2.48301e +000
8.37060e -001	3.40000e -001	1.11729e +000	2.51009e +000
8.43270e -001	3.30000e -001	1.11198e +000	2.53805e +000
8.49480e -001	3.20000e -001	1.10673e +000	2.56694e +000
8.55690e -001	3.10000e -001	1.10157e +000	2.59683e +000
8.61880e -001	3.00000e -001	1.09648e +000	2.62777e +000
8.68060e -001	2.90000e -001	1.09147e +000	2.65985e +000
8.74210e -001	2.80000e -001	1.08655e +000	2.69314e +000
8.80350e -001	2.70000e -001	1.08171e +000	2.72773e +000
8.86450e -001	2.60000e -001	1.07696e +000	2.76372e +000
8.92510e -001	2.50000e -001	1.07230e +000	2.80121e +000
8.98530e -001	2.40000e -001	1.06774e +000	2.84032e +000
9.04500e -001	2.30000e -001	1.06328e +000	2.88120e +000
9.10420e -001	2.20000e -001	1.05891e +000	2.92401e +000
9.16260e -001	2.10000e -001	1.05465e +000	2.96891e +000
9.22040e -001	2.00000e -001	1.05050e +000	3.01611e +000
9.27730e -001	1.90000e -001	1.04646e +000	3.06585e +000
9.33330e -001	1.80000e -001	1.04254e +000	3.11840e +000
9.38820e -001	1.70000e -001	1.03874e +000	3.17408e +000
9.44200e -001	1.60000e -001	1.03507e +000	3.23327e +000
9.49460e -001	1.50000e -001	1.03153e +000	3.29641e +000
9.54580e -001	1.40000e -001	1.02812e +000	3.36405e +000
9.59540e -001	1.30000e -001	1.02486e +000	3.43686e +000
9.64340e -001	1.20000e -001	1.02174e +000	3.51565e +000
9.68950e -001	1.10000e -001	1.01879e +000	3.60147e +000
9.73360e -001	1.00000e -001	1.01599e +000	3.69564e +000
9.77540e -001	9.00000e -002	1.01338e +000	3.79992e +000
9.81490e -001	8.00000e -002	1.01094e +000	3.91670e +000
9.85160e -001	7.00000e -002	1.00870e +000	4.04929e +000
9.88530e -001	6.00000e -002	1.00667e +000	4.20259e +000
9.91570e -001	5.00000e -002	1.00486e +000	4.38414e +000
9.94240e -001	4.00000e -002	1.00329e +000	4.60661e +000
9.96500e -001	3.00000e -002	1.00198e +000	4.89373e +000
9.98280e -001	2.00000e -002	1.00096e +000	5.29875e +000
9.99500e -001	1.00000e -002	1.00027e +000	5.99159e +000
1.00000e +000	0.00000e +000	1.00000e +000	ln(4/g)